



Investigation of ceramic powders using piezoresponse force microscopy[☆]

Nejc Suban^{a,b}, Silvo Drnovšek^a, Hana Uršič^{a,b,*}

^a Electronic Ceramics Department, Jožef Stefan Institute, Jamova 39, 1000 Ljubljana, Slovenia

^b Jožef Stefan International Postgraduate School, Jamova Cesta 39, 1000 Ljubljana, Slovenia

ARTICLE INFO

Keywords:

Perovskite ceramic powder
Piezoelectric
Ferroelectric
Piezoresponse force microscopy
PFM
Sample preparation

ABSTRACT

Piezoresponse force microscopy (PFM) is a widely used technique for probing the piezoelectric and ferroelectric properties of ceramic materials at the nanoscale. However, its application to ceramic powders remains challenging due to the irregular non-flat shape of the powders. In this study, an approach for PFM analysis of ceramic powders is presented, where ceramic powders are embedded in polymer resin and polished to achieve flat surface for PFM imaging. The approach is demonstrated on ferroelectric $\text{PbZr}_{0.53}\text{Ti}_{0.47}\text{O}_3$ (PZT) and $0.65\text{Pb}(\text{Mg}_{1/3}\text{Nb}_{2/3})\text{O}_3-0.35\text{PbTiO}_3$ (PMN-35PT) powders. PFM imaging reveals the piezoelectricity within the powder particles and localises the ferroelectric domains within them, while the PFM switching spectroscopy experiment is used to observe the domain switching behavior.

1. Introduction

Piezoresponse force microscopy (PFM) is a powerful and widely used technique for investigating and quantitative characterization of piezoelectric and ferroelectric properties of ceramic materials at the nanoscale, enabling ferroelectric domains visualization and the study of domain behavior with high spatial resolution [1–3]. In recent years, single crystals [4,5], bulk ceramics, [2,3,6,7], thick [2,8], and thin films [9,10] have been extensively studied using PFM. To some extent, nano objects, such as nanoplates, nanofibers, and nanowires have also been investigated [11,12]. For these nano objects, a common approach involves dispersing them onto substrates [13], often followed by thermal treatment [11] to fix them, making them suitable for PFM analysis. However, studies focusing on the characterization of piezoelectric and ferroelectric nanoparticles and nanopowders [13,14] are less common compared to the other types of ceramic materials mentioned above. This is largely due to several challenges that complicate PFM investigation. Some of the problems include their irregular non-flat shape, weak attachment to the substrate, moving and sticking of the particles to the PFM tip caused by electrostatic interactions during PFM measurements. In this work, we present a method for the reliable and reproducible PFM investigation of irregular non-flat ceramic powders.

2. Experimental

PFM measurements were performed on two ceramic powders with the following compositions: $\text{PbZr}_{0.53}\text{Ti}_{0.47}\text{O}_3$ (PZT) and $0.65\text{Pb}(\text{Mg}_{1/3}\text{Nb}_{2/3})\text{O}_3-0.35\text{PbTiO}_3$ (PMN-35PT). Hereafter, these powders are referred to as PZT and PMN-35PT, respectively. The average particle sizes of PZT and PMN-35PT are $0.51\text{ }\mu\text{m}$ and $0.44\text{ }\mu\text{m}$, respectively, as determined by laser granulometry. Details on the ceramic powders synthesis and X-ray diffraction (XRD) data can be found in the Supplementary Material S1.

To prevent the movement of ceramic powder particles and their sticking to the PFM tip, the powders were fixed using a polymer resin (VersoCit-2, Struers, Denmark). The PZT and PMN-35PT ceramic powders and epoxy resin/hardener mixture were put into a plastic mold in such a way that a very thin layer of resin was first poured into the mold, followed by the powder, and then epoxy resin again on top. After curing, the top surface of the sample was polished using SiC foil (Struers, SiC foil, grit 4000, Denmark), diamond abrasive polishing paste (Struers, DP-paste M $1/4\text{ }\mu\text{m}$, Denmark), and finalized by fine polishing with a colloidal SiO_2 suspension (Struers, Denmark) with particles only a few tens of nanometers in size for approximately 1 min. Further details of the sample preparation procedure are provided in Supplementary Material

[☆] This article is part of a Special issue entitled: 'Perovskite Materials' published in Materials Letters.

* Corresponding author at: Electronic Ceramics Department, Jožef Stefan Institute, Jamova 39, 1000 Ljubljana, Slovenia.

E-mail address: hana.ursic@ijs.si (H. Uršič).

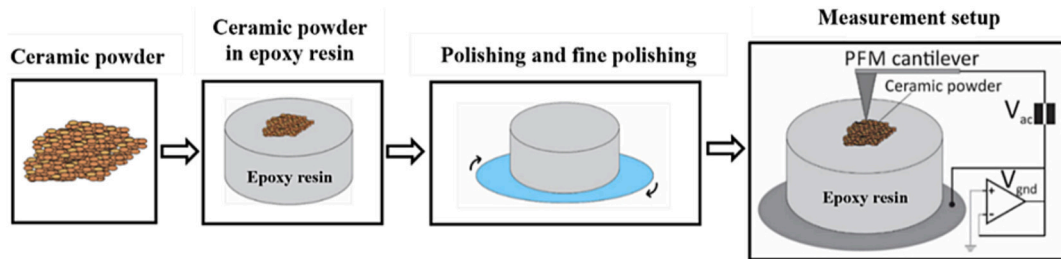


Fig. 1. Schematic of the sample preparation for PFM analysis.

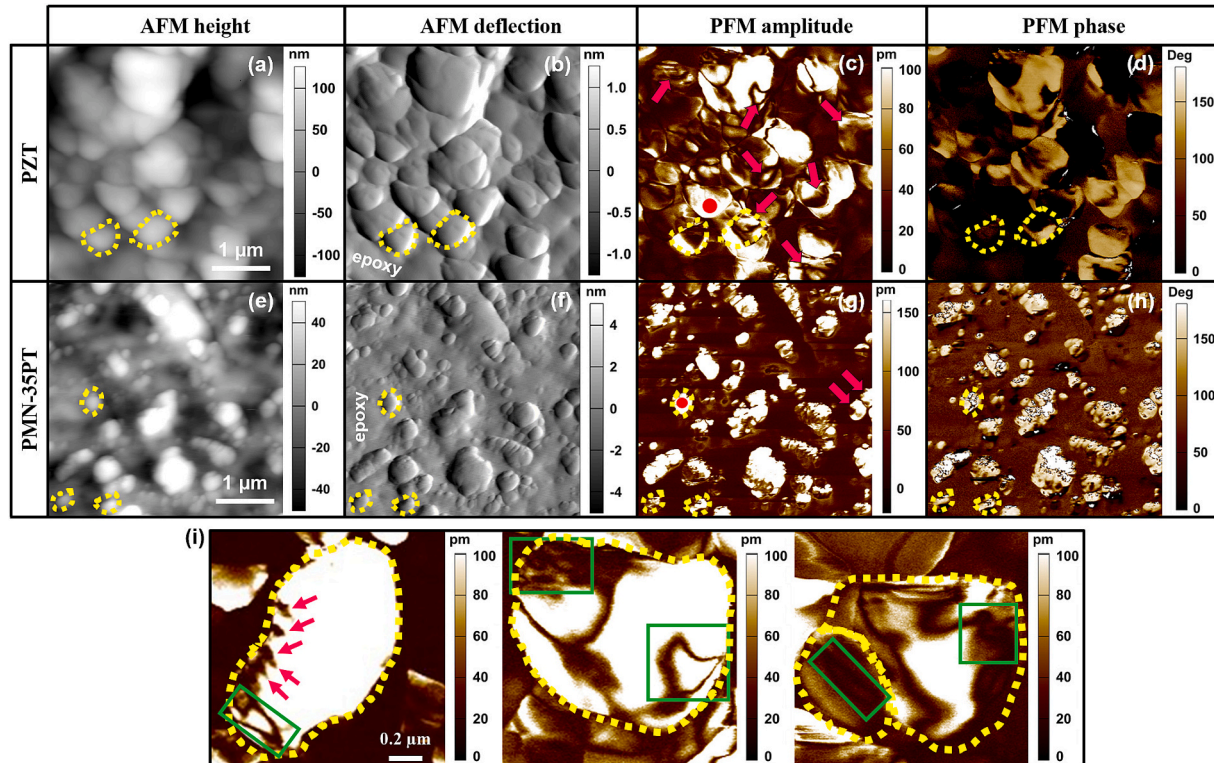


Fig. 2. AFM topography (a, e) and deflection (b, f) images, and vertical PFM amplitude (c, g) and phase (d, h) images, of PZT and PMN-35PT ceramic powders embedded in epoxy resin. (i) Magnified views of PFM amplitude images illustrating the ferroelectric domains in single PZT powder particles. The particle boundaries are marked by yellow dashed lines. Ferroelectric domains are marked with red arrows and green rectangles in panels (c, g, i). (For interpretation of the references to colour in this figure legend, the reader is referred to the web version of this article.)

S2, while the final sample is shown in Supplementary Material S3.

Atomic force microscopy (AFM) and piezoresponse force microscopy (PFM) analyses of ceramic powders were performed using an atomic force microscope (AFM; Asylum Research, MFP-3D, Santa Barbara, CA, USA) equipped with a high-voltage PFM module. For imaging, Ti/Pt coated silicon tips (OMCL-AC240TM-R3, Olympus, Japan) with a tip radius of 25 nm were used. The spring constant (k) and resonance frequency (f) of the cantilever were 2.0 N/m and 70.00 kHz, respectively. Vertical PFM amplitude and phase images were acquired in dual AC resonance tracking (DART) mode by applying an AC voltage of 7 V amplitude at a frequency of ~ 280–310 kHz to the samples. Prior to the PFM measurements, the PFM system was calibrated using periodically poled lithium niobate (PPLN) (see Supplementary Material S4).

After PFM scanning, PFM switching spectroscopy experiments were conducted on the samples. Local PFM amplitude and phase hysteresis loops were measured in PFM switching spectroscopy (SS) off-electric-field mode with a pulsed DC step signal and a superimposed AC drive signal, as described in Ref. [2], to minimize electrostatic contributions. The waveform parameters were as follows: the sequence of rising steps

of the DC electric field was driven at 20 Hz and a maximum amplitude of 100 V; the frequency of the triangular envelope was 0.2 Hz; a superimposed sinusoidal AC signal with an amplitude of 12 V and a frequency of ~ 280 kHz was used. Five cycles were measured in off-electric-field switching spectroscopy mode. PFM experiments were performed in virtual grounding mode (V_{gnd}) at room temperature ($T = 25$ °C). V_{gnd} was previously reported in studies of piezoelectric nanoplates [11] and PMN-35PT films in cross-section [8].

3. Results and discussion

As described in the experimental part, the PZT and PMN-35PT powders were embedded in a polymer resin and polished to obtain a flat surface for PFM scanning. The procedure is schematically shown in Fig. 1.

AFM height and deflection images, PFM out-of-plane amplitude and phase images of PZT and PMN-35PT ceramic powders embedded in the polymer matrix, are shown in Fig. 2. Individual powder particles are observed in the topography height images, with some of them outlined

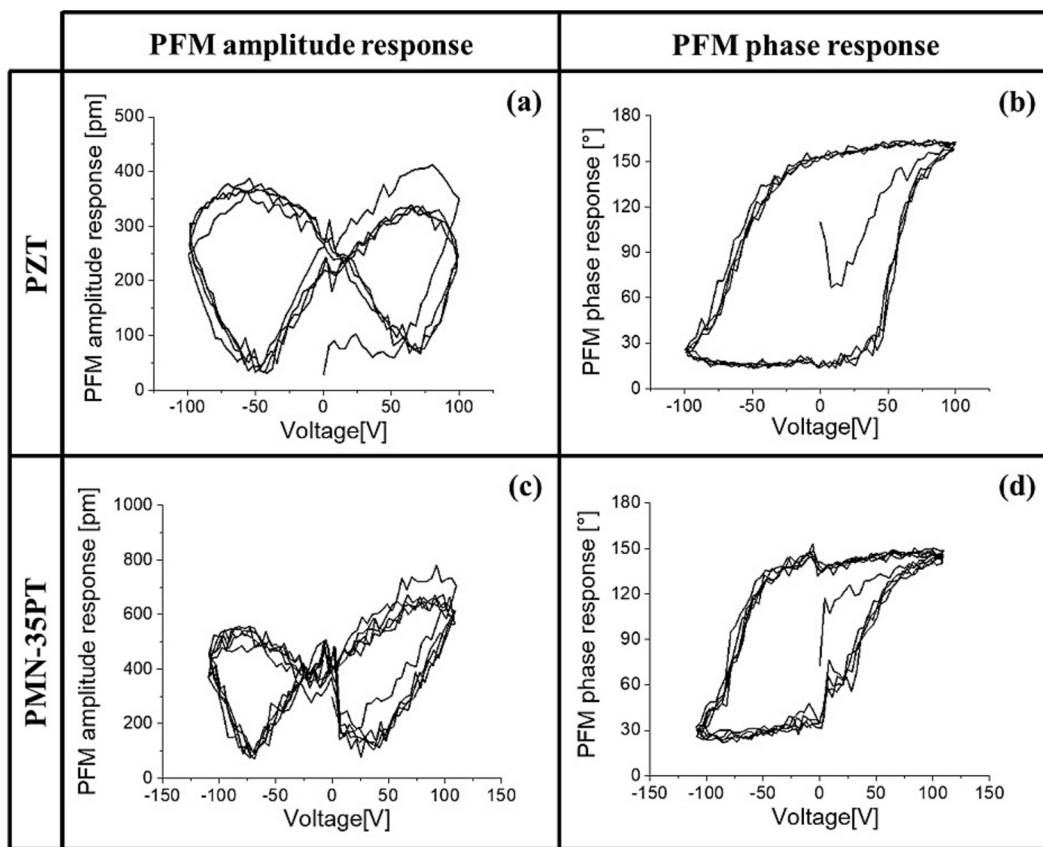


Fig. 3. PFM amplitude and phase hysteresis loops of PZT (a, b) and PMN-35PT (c, d) ceramic powders.

with a yellow dashed line (Fig. 2a and e). It is visible that piezoelectric activity is observed inside the powder. The bright contrast of the PZT and PMN-35PT powder particles in the PFM amplitude images (Fig. 2c and g) indicates their piezoelectric activity compared to the dark brownish contrast of the non-piezoelectric epoxy. In some larger particles, even the ferroelectric domain structure could be observed. Examples of ferroelectric domains are marked with red arrows in the PFM amplitude images in Fig. 2c and g. For better visualization and clarity, Fig. 2i highlights the ferroelectric domain structure within single PZT powder particles. Wedge-shaped and irregular ferroelectric domains can be observed and are marked by red arrows and green rectangles, respectively.

Furthermore, the PFM-SS experiments were conducted to investigate polarization switching within individual ceramic powder particles. Local PFM hysteresis loops were measured at the location marked by a red dot in a Fig. 2c and g. The PFM amplitude and phase loops of PZT and PMN-35PT ceramic powders are presented in Fig. 3. The loops indicate switching of ferroelectric domains within a single powder particle but exhibit asymmetry (Fig. 3c), possibly due to various reasons, namely asymmetric electrode configuration, internal bias, mechanical clamping by the polymer matrix, and electrostatic contributions. Furthermore, crystallographic orientation influences PFM loops shape; unlike textured films, the orientation of ceramic powder particles in the polymer matrix is random, which, according to the literature [15,16], can also lead to asymmetry and variations in loop shape. The experimental data of this work are available in the ref. [17].

4. Conclusions

In this study, we introduce a method for PFM investigation of non-flat particles from piezoelectric/ferroelectric ceramic powders. The

ceramic particles are embedded into the polymer resin and polished to obtain a flat surface for PFM scanning. The feasibility of this approach was successfully demonstrated on perovskite PZT and PMN-35PT powders. Piezoelectric activity and domain switching were observed within individual particle. The developed approach can also be applied to other ferroelectric powders, including emerging lead-free ferroelectric powders, as alternatives to the lead-based materials.

CRediT authorship contribution statement

Nejc Suban: Writing – original draft, Investigation, Data curation. **Silvo Drnovšek:** Investigation. **Hana Ursič:** Writing – original draft, Supervision, Resources, Funding acquisition, Data curation, Conceptualization.

Declaration of competing interest

The authors declare that they have no known competing financial interests or personal relationships that could have appeared to influence the work reported in this paper.

Acknowledgements

This work was supported by the Slovenian Research and Innovation Agency (research project J2-60035, research core funding P2-0105, and Young Researcher project). Jena Cilenšek, Brigita Kmet, and Killian Guillou (Erasmus+ program) are gratefully acknowledged for their help in the laboratory.

Appendix A. Supplementary data

Supplementary data to this article can be found online at <https://doi.org/10.1016/j.matlet.2026.140226>.

Data availability

Research data is uploaded in Zenodo repository

References

- [1] A. Gruverman, M. Alexe, D. Meier, Piezoresponse force microscopy and nanoferroic phenomena, *Nat. Commun.* 10 (2019) 1661, <https://doi.org/10.1038/s41467-019-109650-8>.
- [2] H. Uršić, U. Prah, Investigations of ferroelectric polycrystalline bulks and thick films using piezoresponse force microscopy, *Proc. R. Soc. A.* 475 (2019) 20180782, <https://doi.org/10.1098/rspa.2018.0782>.
- [3] D. Alikin, A. Turygin, A. Kholkin, V. Shur, Ferroelectric domain structure and local piezoelectric properties of lead-free $(\text{K}_{0.5}\text{Na}_{0.5})\text{NbO}_3$ and BiFeO_3 -based piezoelectric ceramics, *Materials* 10 (2017) 47, <https://doi.org/10.3390/ma10010047>.
- [4] V.V. Shvartsman, A.L. Kholkin, Polar structures of $\text{PbMg}_{1/3}\text{Nb}_{2/3}\text{O}_3\text{-PbTiO}_3$ relaxors: piezoresponse force microscopy approach, *J. Adv. Dielectr.* 2 (2012) 1241003, <https://doi.org/10.1142/S2010135X12410032>.
- [5] D. Zhang, L. Wang, L. Li, P. Sharma, J. Seidel, Varied domain structures in 0.7Pb $(\text{Mg}_{1/3}\text{Nb}_{2/3})\text{O}_3\text{-}0.3\text{PbTiO}_3$ single crystals, *Microstructures* 3 (2023) 2023046, <https://doi.org/10.20517/microstructures.2023.57>.
- [6] H. Uršić, A. Benčan, U. Prah, M. Dragomir, B. Malic, Structure and dynamics of ferroelectric domains in polycrystalline $\text{Pb}(\text{Fe}_{1/2}\text{Nb}_{1/2})\text{O}_3$, *Materials* 12 (2019) 1327, <https://doi.org/10.3390/ma12081327>.
- [7] S. Xie, Q. Xu, Q. Chen, J. Zhu, Q. Wang, Realizing super-high piezoelectricity and excellent fatigue resistance in domain-engineered bismuth Titanate ferroelectrics, *Adv. Funct. Mater.* 34 (2024) 2312645, <https://doi.org/10.1002/adfm.202312645>.
- [8] H. Uršić, M. Šadi, Investigation of piezoelectric $0.65\text{Pb}(\text{Mg}_{1/3}\text{Nb}_{2/3})\text{O}_3\text{-}0.35\text{PbTiO}_3$ films in cross section using piezo-response force microscopy, *Appl. Phys. Lett.* 121 (2022) 192905, <https://doi.org/10.1063/5.0104829>.
- [9] K. Hond, M. Salvareda, M. Ahmadi, E. Houwman, B. Noheda, B.J. Kooi, G. Rijnders, G. Koster, Structural properties of $\text{Hf}_{0.5}\text{Zr}_{0.5}\text{O}_2$ integrated on silicon, *ACS Appl. Electron. Mater.* 7 (2025) 8013–8019, <https://doi.org/10.1021/acsaelm.5c00753>.
- [10] L. Dai, Y. Xie, B. Wang, J. Long, H. Shen, P. Jiang, X. Zhong, G. Zhong, Flexible freestanding $\text{PbZr}_{0.2}\text{TiO}_{0.8}\text{O}_3$ ferroelectric thin films with stable and tunable domain configuration, *Mater. Today Commun.* 48 (2025) 113625, <https://doi.org/10.1016/j.mtcomm.2025.113625>.
- [11] M.M. Kržmanc, H. Uršić, A. Meden, R.C. Korošec, D. Suvorov, $\text{Ba}_{1-x}\text{Sr}_x\text{TiO}_3$ plates: synthesis through topochemical conversion, piezoelectric and ferroelectric characteristics, *Ceram. Int.* 44 (2018) 21406–21414, <https://doi.org/10.1016/j.ceramint.2018.08.198>.
- [12] T. Jalabert, M. Pusty, M. Mouis, G. Ardila, Investigation of the diameter-dependant piezoelectric response of semiconducting ZnO nanowires by Piezoresponse Force Microscopy and FEM simulations 34 (2023) 15402, <https://doi.org/10.1088/1361-6528/acac35>.
- [13] R.K. Vasudevan, K.A. Bogle, A. Kumar, S. Jesse, R. Magaraggia, R. Stamps, S. B. Ogale, H.S. Potdar, V. Nagarajan, Ferroelectric and electrical characterization of multiferroic BiFeO_3 at the single nanoparticle level, *Appl. Phys. Lett.* 99 (2011) 252905, <https://doi.org/10.1063/1.3671392>.
- [14] M.E. Castillo, V.V. Shvartsman, D. Gobeljic, Y. Gao, J. Landers, H. Wende, D. C. Lupascu, Effect of particle size on ferroelectric and magnetic properties of BiFeO_3 nanopowders, *Nanotechnology* 24 (2013) 355701, <https://doi.org/10.1088/0957-4484/24/35/355701>.
- [15] E. Leal-Perez, J. Flores-Valenzuela, J.L. Almaral-Sánchez, S.F. Oliver-Mendez, M. P. Cruz, O. Auciello, A. Hurtado-Macias, Piezoelectric and nanomechanical properties of lead-free $\text{K}_{0.1}\text{Na}_{0.9}\text{Nb}_{0.97}\text{Sb}_{0.03}\text{O}_3$ (KNNS) thin films grown by radio frequency sputtering, *J. Eur. Ceram. 43 (2023) 7431–7439*, <https://doi.org/10.1016/j.jeurceramsoc.2023.07.064>.
- [16] C.J. Ramos-Cano, M. Miki-Yoshida, R. Herrera-Basurto, F. Mercader-Trejo, L. Fuentes-Cobas, O. Auciello, A. Hurtado Macías, Effect of the orientation polarization and texturing on nano-mechanical and piezoelectric properties of PZT (52/48) films, *Appl. Phys. A Mater. Sci. Process.* 129 (2023) 16, <https://doi.org/10.1007/s00339-022-06374-3>.
- [17] N. Suban, H. Uršić, Zenodo, 2025, Doi: <https://doi.org/10.5281/zenodo.17377465>